Journal of Geophysical Research – Solid Earth

Supporting Information for

Earthquake Interactions in Central Taiwan:
Probing Coulomb stress effects due to $M_L \geq 5.5$ earthquakes from 1900 to 2017

Shanshan Li[1], Shimon Wdowinski[1], Ya-Ju Hsu[2], J. Bruce H. Shyu[3]

[1] Institute of Environment, Department of Earth and Environment, Florida International University, Miami, Florida, USA.

[2] Institute of Earth Sciences, Academia Sinica, P.O. Box 1–55, Nankang, Taipei, Taiwan.

[3] Department of Geosciences, National Taiwan University, Taipei, Taiwan.

Contents of this file

Additional Supporting Information (Files uploaded separately)

Figure S1
Figure S2

Introduction

This support information includes two text sections (S1 and S2), nine figures (Figures S1 to S9) and six tables (Tables S1 to S6). The two text sections describe potential stress influence from (1) large magnitude earthquakes with $M_L \geq 6.0$ which are located outside of our study area but not far away from the mainshocks in the Central-Taiwan-Mainshock sequence and (2) the 1999 postseismic cumulative afterslip over 14 years. The nine figures describe stress evolution on nearby fault systems due to preceding earthquakes, detailed results about exploring sensitivity of source slip models, receiver fault geometry (strike, dip and rake angles), location of hypocenter for the receiver fault and effective friction coefficient on the calculated Coulomb stress changes

(ΔCFSs) and ΔCFS on active faults due to large earthquakes outside of our study area and postseismic effect. The six tables provide fault parameters of source faults and receiver faults used in our paper, statistical results about the sensitivity analysis and calculated ΔCFS at hypocenters of subsequent mainshocks due to large earthquakes outside of our study area and 1999 Chi-Chi postseismic cumulative afterslip.

Text Sections

S1. ΔCFS on hypocenters of subsequent mainshocks due to earthquakes located outside of our study area but not far from the Central-Taiwan-Mainshock earthquake sequence

In order to explore possible influence of other major earthquakes that are not included within our main study but are located not far from the Central-Taiwan-Mainshock earthquake sequence and active faults, we conducted an additional analysis of 9 additional ($M_L \geq 6.0$) events located outside of the study area (orange circles in Figure S7, Table S4). As in the main analysis described in section 3 of the main text, we calculated ΔCFS at hypocenters of the mainshocks in the Central-Taiwan-Mainshock earthquake sequence (Table 1) after each one of 9 additional events (Table S4). In this analysis, mainshocks in the Central-Taiwan-Mainshock earthquake sequence are the receiver faults and the 9 additional events are the source faults. The additional analysis reveal ΔCFSs at the hypocenters of the mainshocks in the sequence due to 9 events outside of our study area are in the range of -0.20 bar to 0.35 bars (Table S5). Only magnitude changes in ΔCFS have been found at hypocenters of mainshocks in the sequence and stress states (status of promotion or inhibition) of those mainshocks did not change at all. Except for the 2016 Meinong mainshock, ΔCFS due to preceding 42 earthquakes in our study area was already the threshold 0.1 bar. Adding stress effects of the 9 extra events and uncertainty of Coulomb stress analysis make the stress status of 2016 mainshock more questionable. We also calculated ΔCFS on nearby fault systems due to 9 events located outside of our study area. There are only magnitude changes in ΔCFS for all fault patches of nearby fault systems after adding those 9 events in a range of -0.90 bar to 1.80 bars. Stress effect from those 9 additional events did not change our conclusion about the stress states (promoted or inhibited) on active faults in the main text (Figure S8).

S2. Coulomb stress effect of 14 years of cumulative afterslip for 1999 Chi-Chi earthquake at hypocenters of Central-Taiwan-Mainshock earthquake sequence and on active faults

Using 14 years of Global Positioning System (GPS) observations following the 1999 Chi-Chi earthquake, Tang et al. (2019) demonstrated a notable cumulative afterslip of ~ 1 m on the southern segment of the Chelungpu fault which is not the same place that has large coseismic slip during the Chi-Chi event. In order to investigate potential stress effect of postseismic deformation of the 1999 Chi-Chi earthquake, we calculated ΔCFSs at hypocenters of subsequent mainshocks and on 8 active faults (Tables 1 and 2) due to 14 years of cumulative afterslip (Tang et al. 2019). We first calculated ΔCFS for each mainshock happened after 1999 Chi-Chi earthquake in the Central-Taiwan-Mainshock earthquake sequence, which includes the 2009 Nantou, 2010 Jiashian, two 2013 Nantou and 2016 Meinong earthquakes. In this Coulomb stress analysis model, we assigned each mainshock as receiver fault and cumulative afterslip as source fault which includes years of afterslip from 1999 Chi-Chi to the time when each subsequent mainshock happened. For 2016 Meinong earthquakes, we use all 14 years of cumulative afterslip since this mainshock happened at about 17 years after the occurrence of 1999 Chi-Chi event. The calculated ΔCFSs at hypocenters of subsequent mainshocks reveal that: (1) stress influence from cumulative postseismic afterslip is about 3– 27% of the coseismic effect; (2) only magnitude change have been found in the calculated ΔCFSs at hypocenters; (3) including the 1999 postseismic effect did not change the stress states (promoted or inhibited) at hypocenters; (4) stress state at hypocenter of 2016 Meinong earthquake is still questionable since postseismic effect is minor and the calculated ΔCFS is the triggering threshold 0.10 bar (Table S6).

We also calculated ΔCFS on 8 active faults (Table 2) due to 14 years of cumulative postseismic afterslip and evaluated with the values due to coseismic effects of preceding earthquakes from 1900 – 2017. This Coulomb analysis model indicates that magnitude changes in ΔCFSs have been found on the Chelungpu, Shungtung, Changhua faults and flat decollement of Central Taiwan after considering the 1999 postseismic afterslip effect. The stress states of fault patches on Chelungpu, Shungtung, Changhua faults and most area on the flat decollement are not changing. We found only a small area of fault patches within middle part of flat decollement experience sign changes in ΔCFSs. In order to better illuminate magnitude and/or sign changes in calculated ΔCFS resulted from the 1999 postseismic cumulative afterslip, we select three areas on flat decollement from updip to downdip (black ellipses a, b and c in Figure S9). Within ellipse ***a*** in Figure S9 which is located along updip side of flat decollement, stress states of fault patches did not change with only magnitude changes in ΔCFS in a range of -10 to 14 bars. Similar with ellipse ***a***, only magnitude changes in ΔCFS in a range of -3.23 bar to 0.76 bar have been found for fault patches within ellipse ***c*** which is located downdip side of flat decollement (Figure S9). Whereas within ellipse ***b***, most fault patches experience only magnitude change in ΔCFS in a range of -32.2 to 58.1 bars except stress states of 7 out of 50 fault patches changed from promotion to inhibition which located sparsely in the middle part of flat decollement. In summary, the 1999 postseismic afterslip did change stress states for a very small area in the middle part of flat decollement but did not change our conclusion that flat decollement of Central Taiwan was promoted by preceding earthquakes. We also found that although only a small area changes the stress state, the afterslip-induced stress change on active faults is very large compared to the triggering threshold $\pm$0.1 bar, which indicates the importance of considering stress influence from the postseismic afterslip.

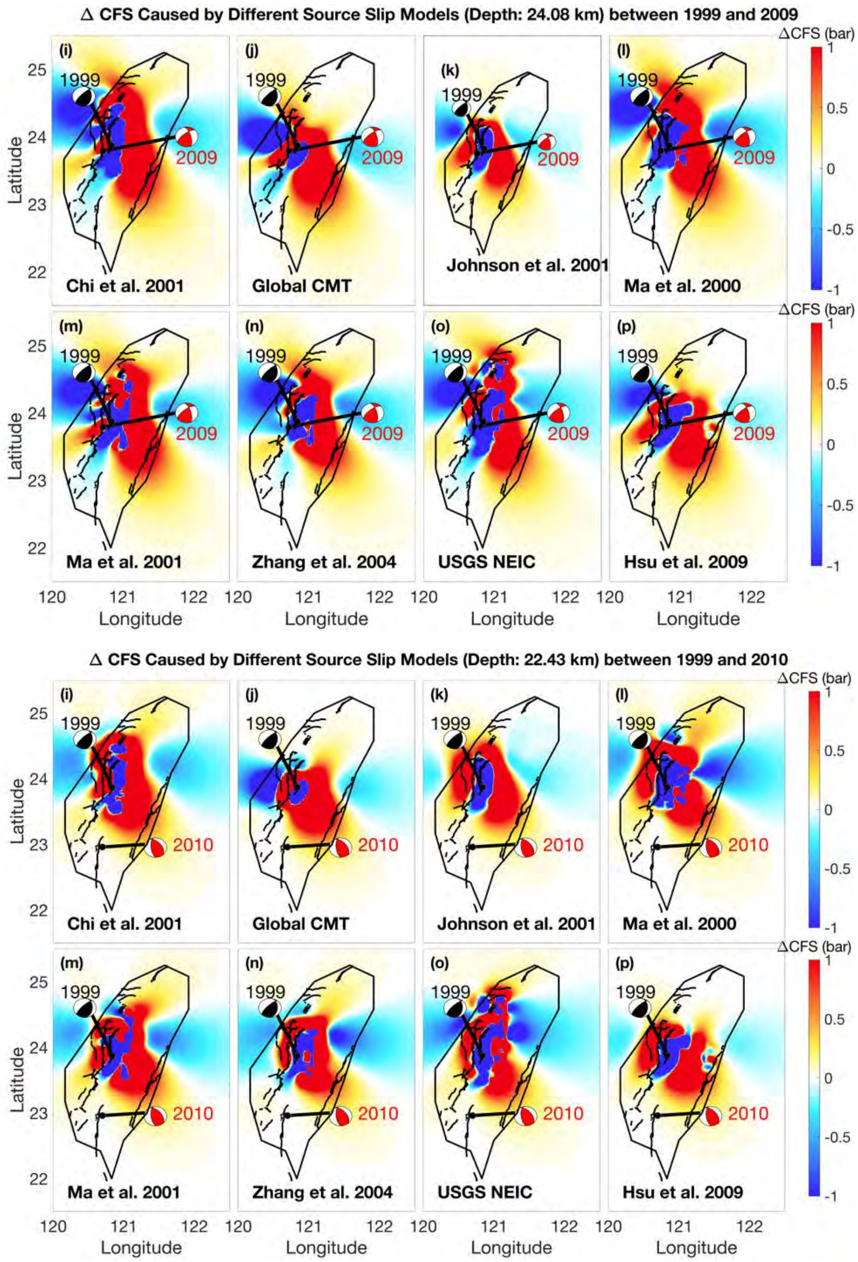

Figure S3. Coseismic Coulomb stress changes caused by different source slip models of the 1999 Chi-Chi earthquake on the receiver fault which has the same fault parameter as the 2009 Nantou earthquake ((a) – (h)) and the 2010 Jiashian earthquake ((i) – (p)). The source of each slip model is marked in black bold text within each subfigure. For subfigures (a) – (h), the black beachball represents the 1999 Chi-Chi earthquake (9/20/1999), the red beachball represents the 2009 Nantou earthquake (11/5/2009). For subfigures (i) – (p), the black beachball represents the 1999 Chi-Chi earthquake (9/20/1999), the red beachball represents the 2010 Jiashian earthquake (3/4/2010).

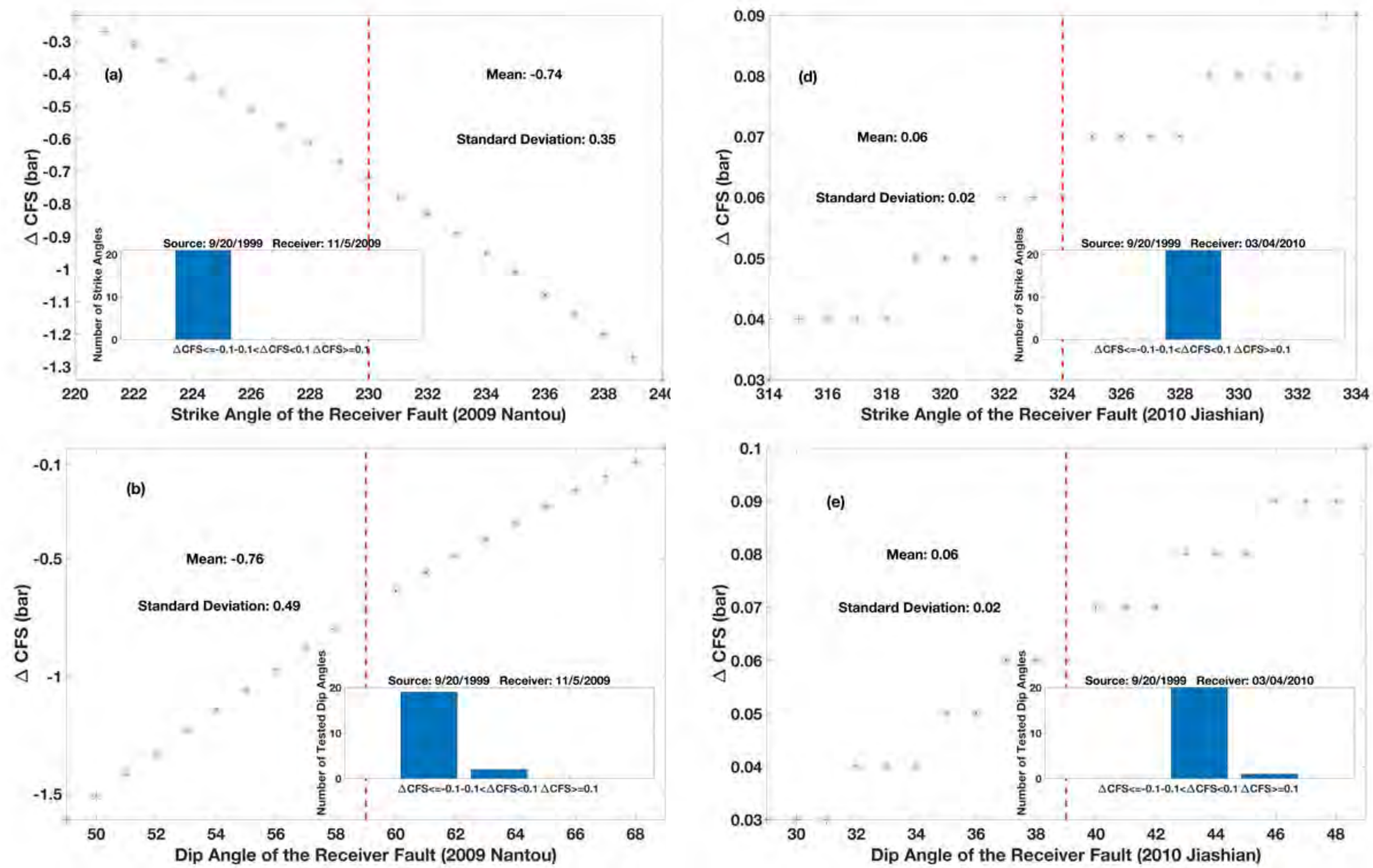

Figure S4. Sensitivity of the ΔCFSs due to strike and dip angles of the receiver fault for the 2009 Nantou ((a) – (b)) and the 2010 Jiashian ((d)-(e)). Histogram in the inset of each subfigure shows distribution of calculated ΔCFSs in three bins: ΔCFS ≥ 0.1 bar, ΔCFS ≤ -0.1 bar and -0.1 < ΔCFS < 0.1 bar.

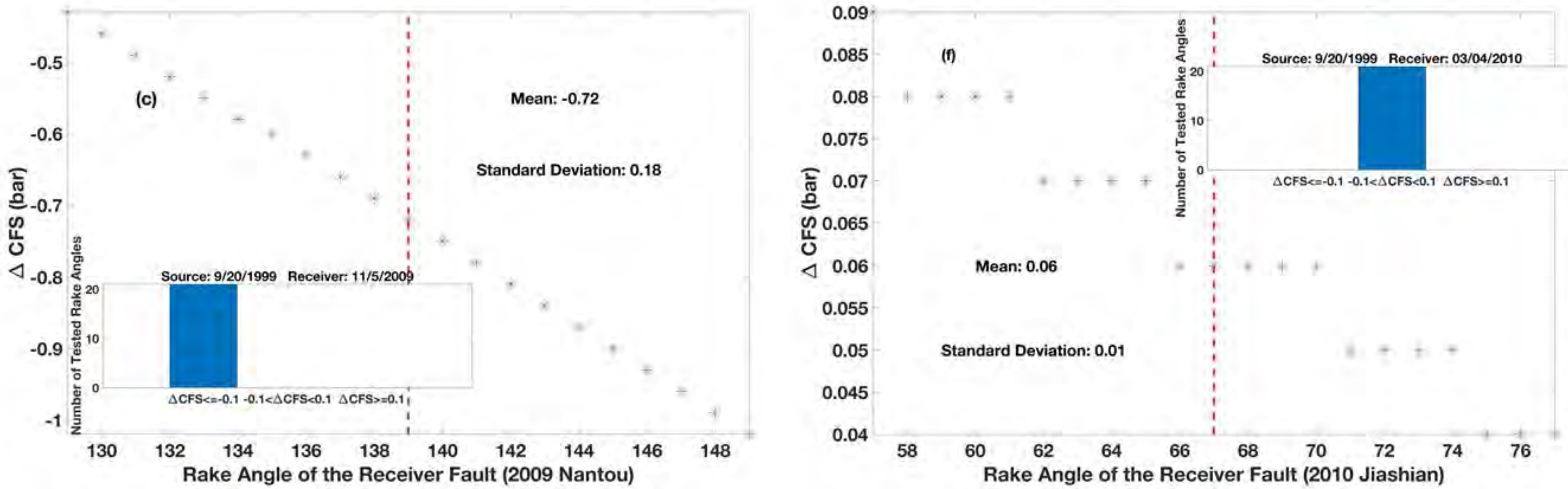

Figure S4. (continued) Sensitivity of the ΔCFSs due to variation of rake angles of the receiver fault for the 2009 Nantou (c) and the 2010 Jiashian (f). Histogram in the inset of each subfigure shows distribution of calculated ΔCFSs in three bins: ΔCFS ≥ 0.1 bar, ΔCFS ≤ -0.1 bar and -0.1 < ΔCFS < 0.1 bar.

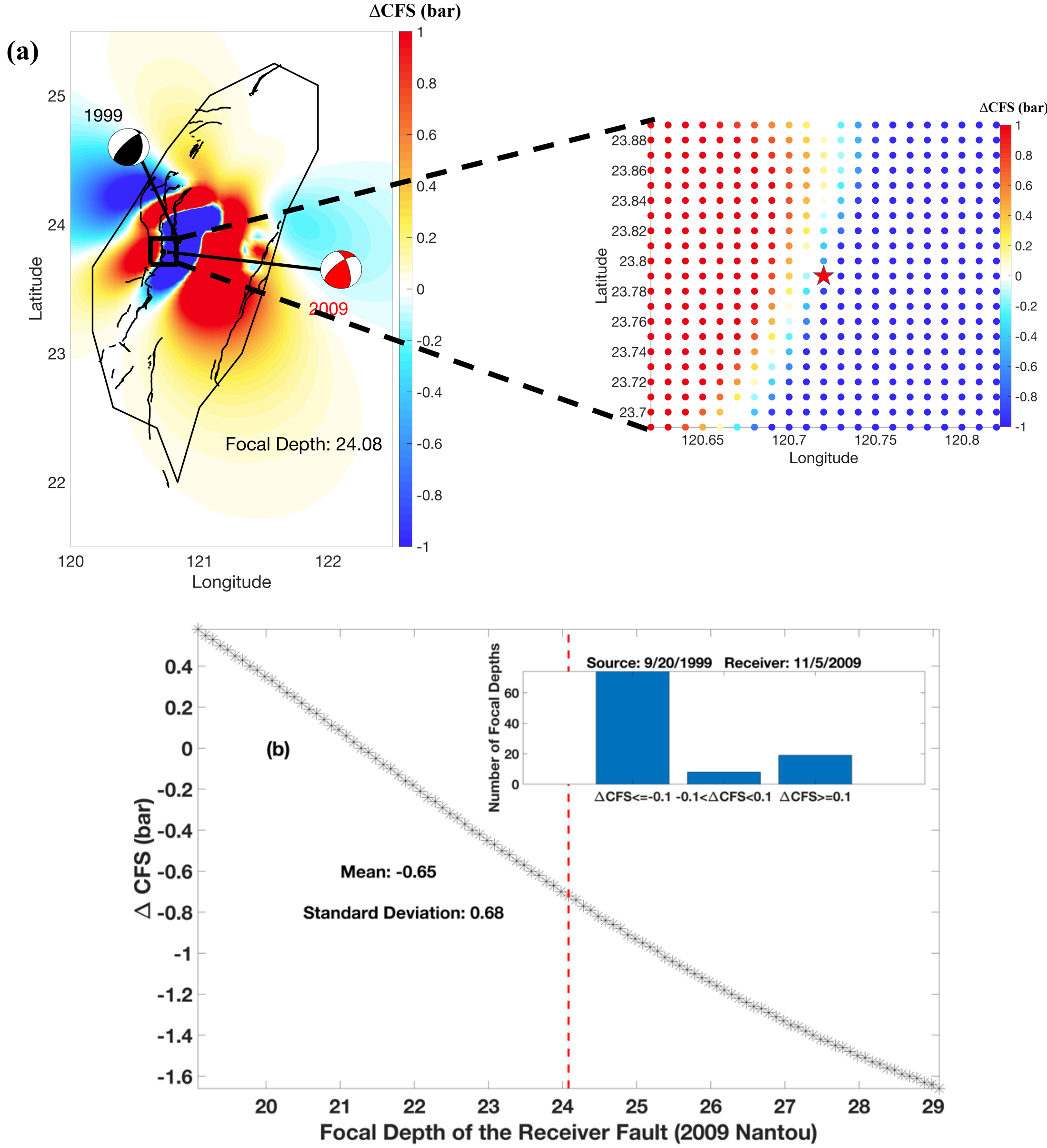

Figure S5. The sensitivity test of the variation in location of hypocenters of the 2009 Nantou mainshock ((a) – (b)). (a) shows the sensitivity of the calculated ΔCFSs due to variation of the epicenter with focal depth fixed. The black box in (a) is $0.2^o \times 0.2^o$ and the center is the epicenter of the 2009 Nantou earthquake (marked as red star). (b) shows sensitivity result of calculated ΔCFSs at the hypocenter due to variation of the focal depth with epicenter fixed. Histogram in the inset of (b) shows distribution of calculated ΔCFSs in three bins: ΔCFS ≥ 0.1 bar, ΔCFS ≤ -0.1 bar and -0.1 < ΔCFS < 0.1 bar.

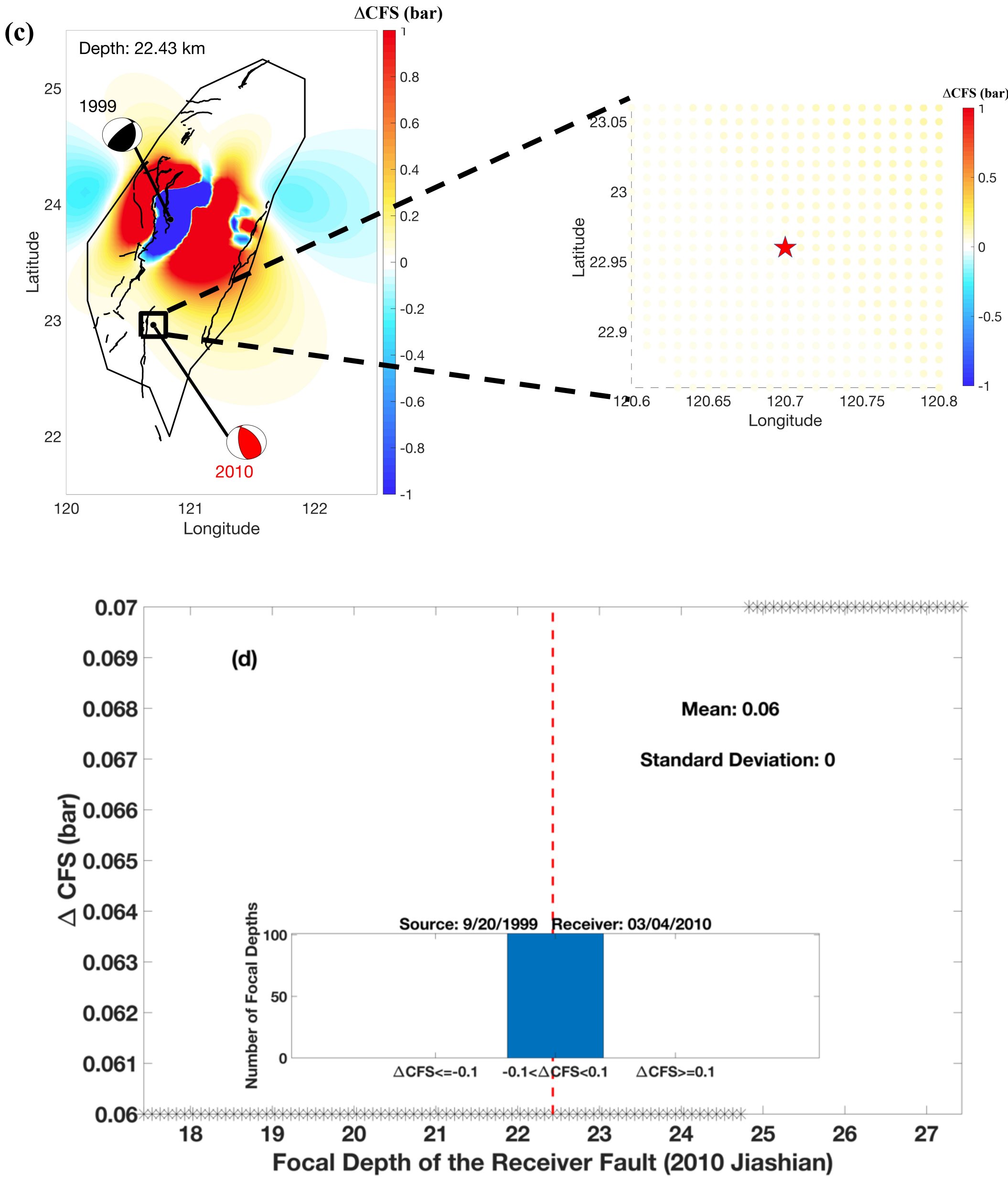

Figure S5. (continued) The sensitivity test of the variation in location of hypocenters of the 2010 Jiashian mainshock ((c) – (d)). (c) shows the sensitivity of the calculated ΔCFSs due to variation of the epicenter with focal depth fixed. The black box in (c) is $0.2^{o} \times 0.2^{o}$ and the center is the epicenter of the 2010 Jiashian earthquake (marked as red star). (d) shows sensitivity result of calculated ΔCFSs at the hypocenter due to variation of the focal depth with epicenter fixed. Histogram in the inset of (d) shows distribution of calculated ΔCFSs in three bins: ΔCFS ≥ 0.1 bar, ΔCFS ≤ -0.1 bar and -0.1 < ΔCFS < 0.1 bar.

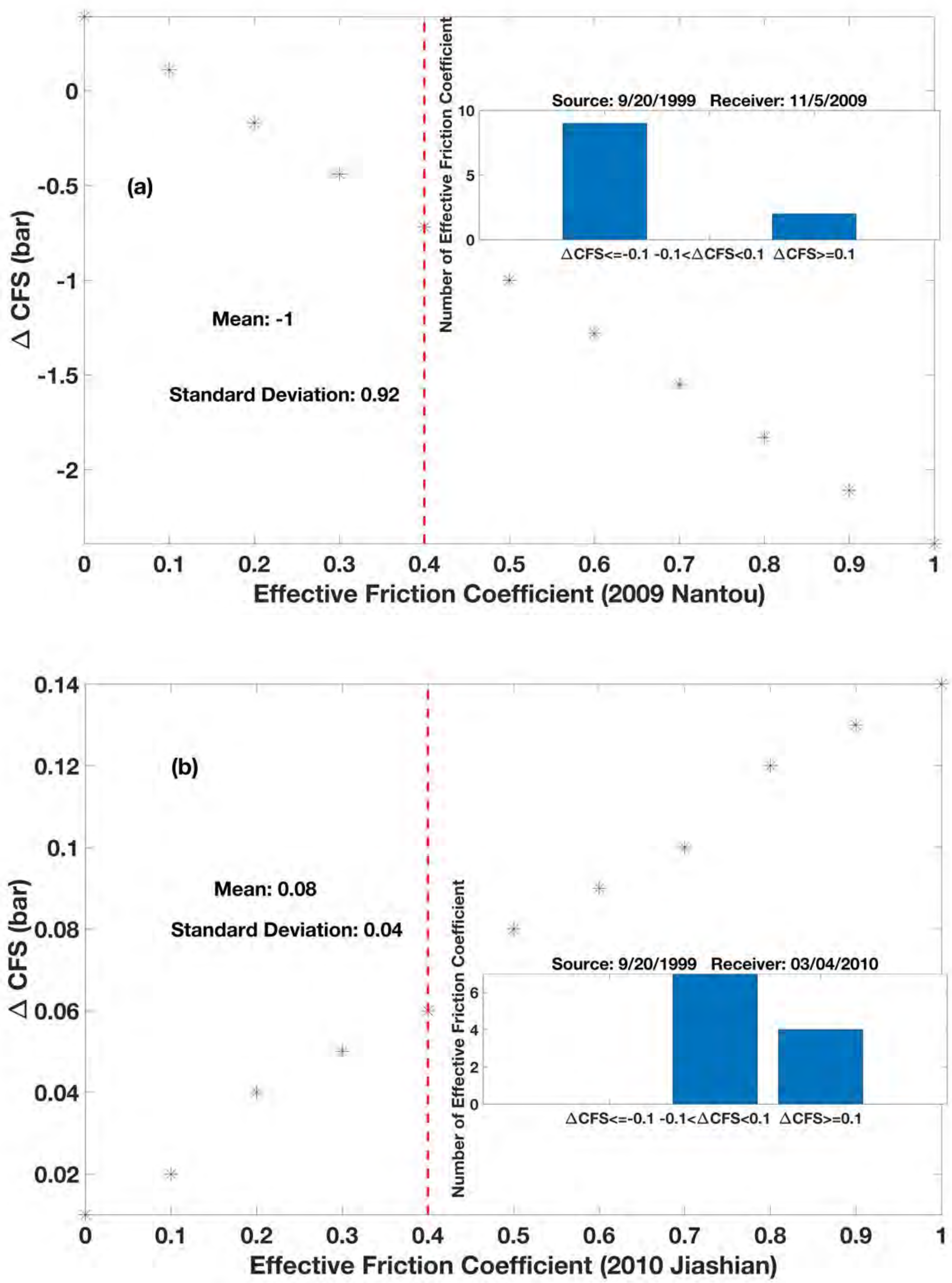

Figure S6. Sensitivity Test for the variation of the effective friction coefficient (μ') (a) and (b). (a) The receiver fault geometry is 230/59/139. (b) The receiver fault geometry is 324/39/67. Histograms in the inset of (a) and (b) show distribution of calculated ΔCFSs in three bins: ΔCFS ≥ 0.1 bar, ΔCFS ≤ -0.1 bar and -0.1 < ΔCFS < 0.1 bar.

1	3/16/1906
2	4/20/1935
3	12/16/1941
4	12/4/1946
5	1/18/1964
6	11/9/1972
7	5/11/1983
8	7/17/1998
9	9/20/1999
10	11/5/2009
11	3/4/2010
12	3/27/2013
13	6/2/2013
14	2/5/2016

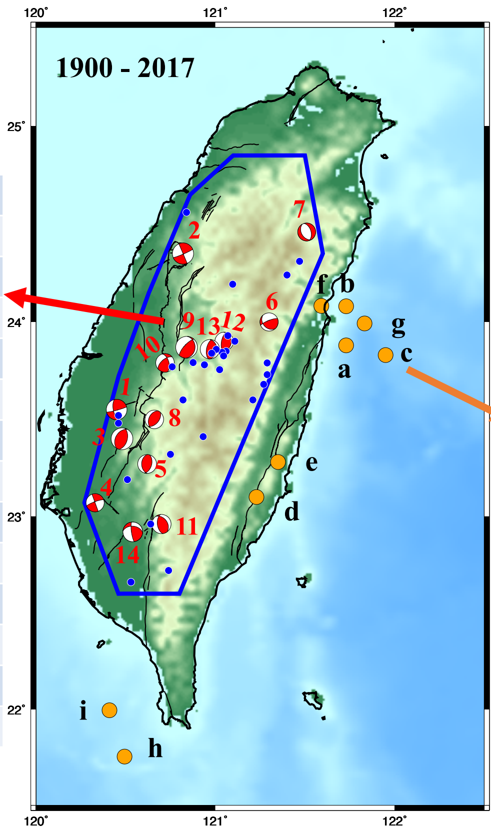

a	10/21/1951
b	10/22/1951 03:29:31
c	110/22/1951 05:42:58
d	11/24/1951 18:47:23
e	11/24/1951 18:50:30
f	05/20/1986
g	11/14/1986
h	12/26/2006 12:26:20.9
i	12/26/2006 12:34:14.7

Figure S7. Location map of earthquakes used in the additional ΔCFS analysis described in Text S1. Earthquakes (1) - (14) represent the 14 targeted mainshocks in the Central-Taiwan-Mainshock sequence. Earthquakes (a) – (i) represent the 9 events outside of the blue polygon which is our area of interest. Red beachballs and blue points are the same meaning as the ones in Figure 1b.

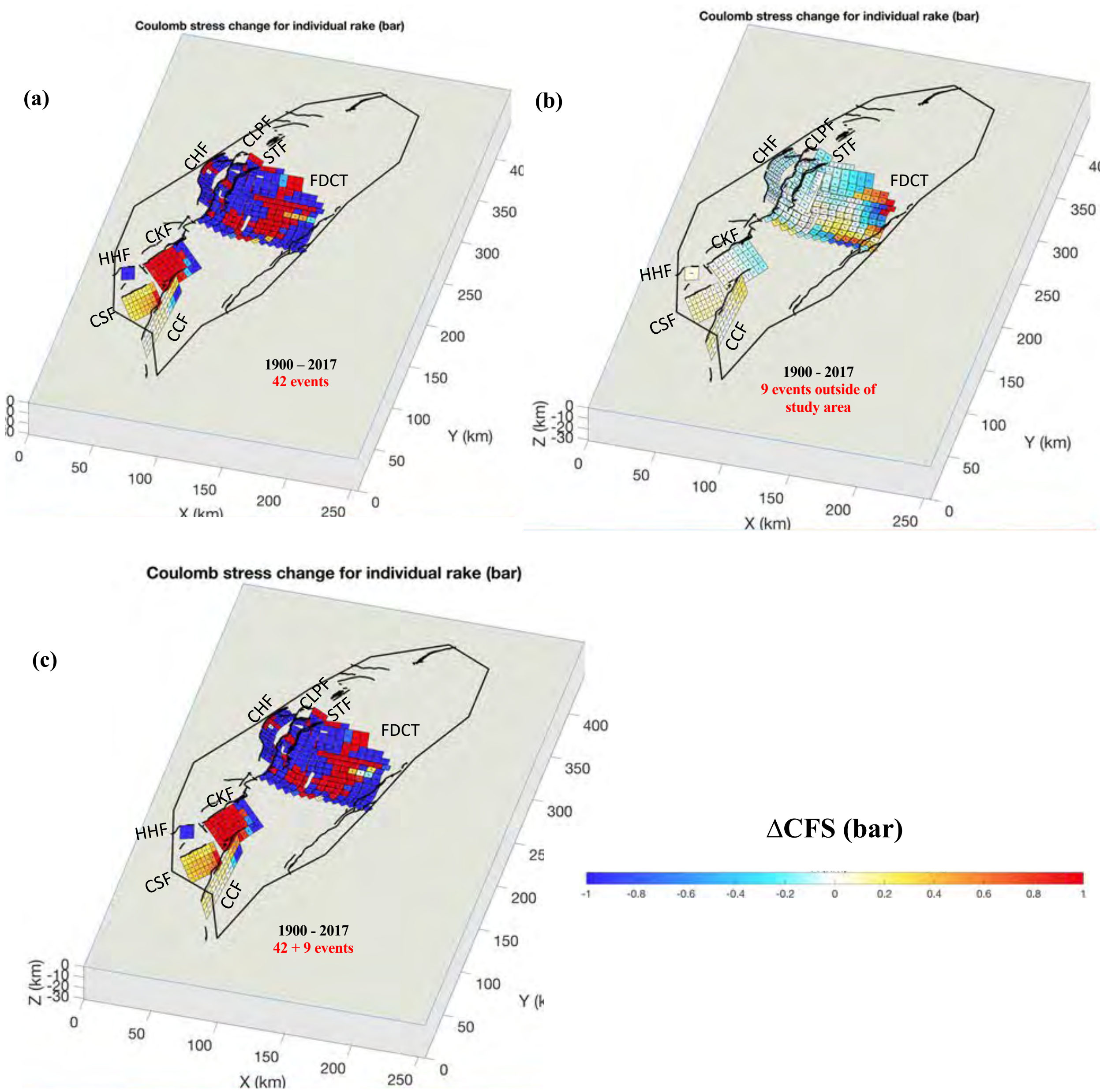

Figure S8. Coulomb stress change on active faults due to preceding 42 events within study area (a), due to 9 additional events outside of our study area (b) and due to 51 (42+9) events in total. CHF: Changhua Fault; CLPF: Chelungpu Fault; STF: Shungtung fault; FDCT: Flat Decollement of Central Taiwan; CKF: Chukou Fault; HHF: Hsinghua Fault; CCF: Chaochou Fault; CSF: Chishan Fault.

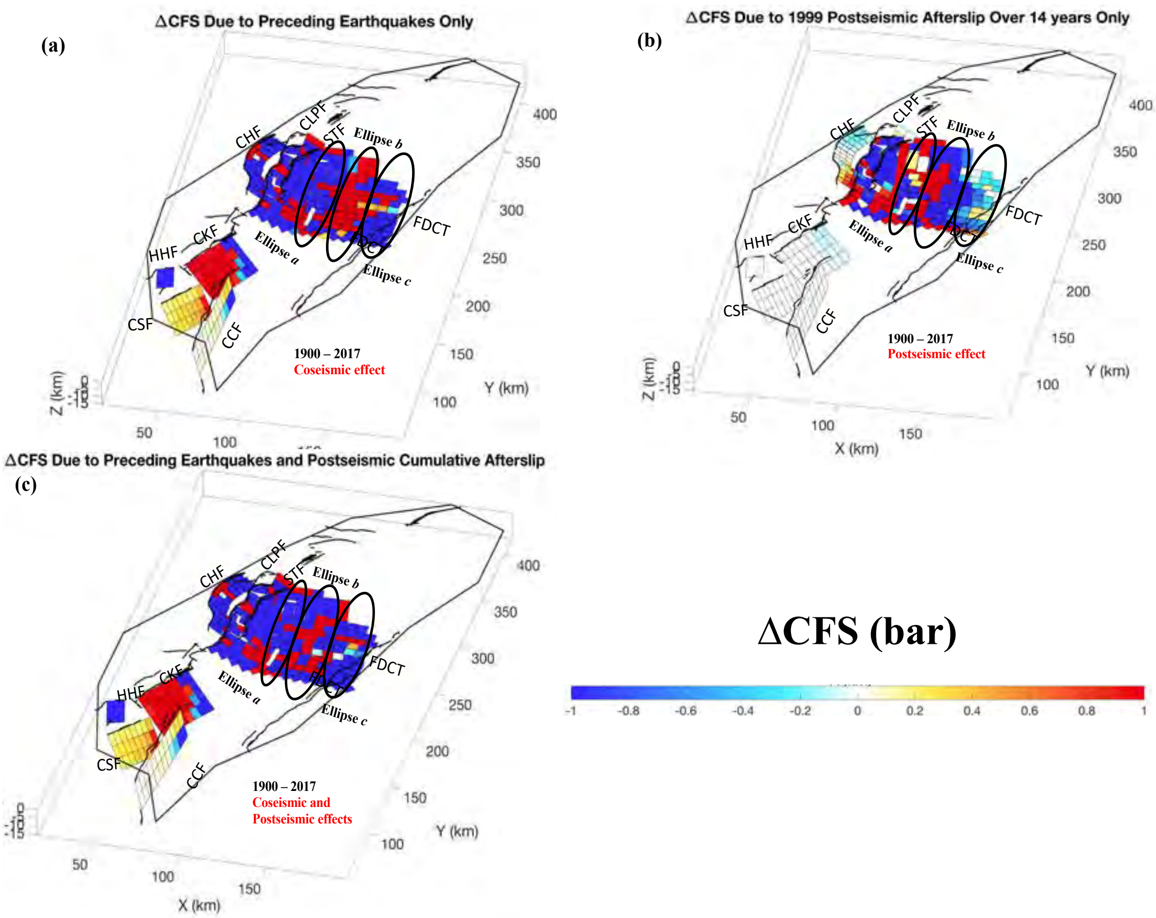

Figure S9. Coulomb stress change on active faults due to coseismic rupture of preceding 42 events within study area (a), due to 14 years of 1999 Chi-Chi postseismic cumulative afterslip (b) and coseismic and postseismic effect s in total (c). CHF: Changhua Fault; CLPF: Chelungpu Fault; STF: Shungtung Fault; FDCT: Flat Decollement of Central Taiwan; CKF: Chukou Fault; HHF: Hsinghua Fault; CCF: Chaochou Fault; CSF: Chishan Fault.

Table S1. Fault parameters of all source faults used in this study including 14 mainshocks in the Central-Taiwan-Mainshock sequence and 28 other surrounding earthquakes which are not in the sequence in Central Taiwan from 1900 to 2017. L: fault length in km. W: fault width in km. Unit of netslip is meter. “CWBSN” in the reference list indicates the location of the earthquake has obtained from the Central Weather Bureau Seismic Network. “CMT” indicates the focal mechanism information obtained from the global CMT catalog for specific earthquake. “BATS” stands for Broadband array in Taiwan for Seismology. Ref.: 1. (Liao et al. 2018); 2. (Lin et al. 2013); 3. (Lin & Xiao, 2004); 4. (Hsu et al. 2011); 5. (CWBSN, Kao et al., 2000); 6. (CWBSN, Wu, 1978); 7. (CWBSN, CMT); 8. (CWBSN, Ma & Wu, 2001); (9). (Hsu et al. 2009); (10). (CWBSN, Hsu et al., 2011); (11) (Lee et al., 2015); (12). (Lee et al., 2015); (13). (CWBSN, Wen et al., 2017); 14. (CMT); 15. (Ma & Wu, 2001); 16. (CWBSN); 17. (BATs); 18. (BATs, CMT).

No.	Date	Lon	Lat	Depth	Strike	Dip	Rake	Fault Patch			M	Ref.
								L	W	netslip		
		Followings are 14 mainshocks in the sequence										
1	**1906/3/16**	**variable slip distribution on 3D fault-geometry from Liao et al. 2018 (see data repository)**									**6.9**	**1**
2	**1935/4/20**	**variable slip distribution on 3D fault-geometry from Lin et al. 2013 (see data repository)**									**7.1**	**2**
3	**1941/12/16**	**variable slip distribution on 3D fault-geometry from Lin and Xiao, 2004 (see data repository)**									**7.3**	**3**
4	**1946/12/4**	**120.33**	**23.07**	**5**	**250**	**80**	**180**	**15.4**	**7.7**	**0.439**	**6.1**	**4**
5	**1964/1/18**	**120.62**	**23.27**	**18**	**15**	**50**	**100**	**6.5**	**4.8**	**0.421**	**6.3**	**5**
6	**1972/11/9**	**121.3**	**24**	**10**	**137**	**33**	**155**	**10.3**	**6.8**	**0.524**	**6.1**	**6**
7	**1983/5/11**	**121.51**	**24.46**	**1.23**	**150**	**40**	**-100**	**7.6**	**6.1**	**0.281**	**6.0**	**7**
8	**1998/7/17**	**variable slip distribution on 3D fault-geometry from Ma and Wu, 2001 (see data repository)**									**6.2**	**8**
9	**1999/9/20**	**variable slip distribution on 3D fault-geometry from Hsu et al. 2009 (see data repository)**									**7.3**	**9**
10	**2009/11/5**	**120.72**	**23.79**	**24.08**	**230**	**59**	**139**	**12.0**	**7.7**	**0.563**	**6.2**	**7**
11	**2010/3/4**	**120.7**	**22.96**	**22.43**	**324**	**39**	**67**	**16.4**	**9.8**	**0.651**	**6.4**	**10**
12	**2013/3/27**	**121.05**	**23.90**	**19.4**	**355**	**25**	**75**	**10.3**	**6.8**	**0.524**	**6.2**	**11**
13	**2013/6/2**	**120.97**	**23.86**	**14.5**	**2**	**29**	**83**	**16.4**	**9.8**	**0.651**	**6.5**	**12**
14	**2016/2/5**	**120.54**	**22.92**	**15.3**	**275**	**42**	**17**	**19.1**	**11.0**	**0.700**	**6.6**	**13**

Table S1. (continued) Fault parameters of all source faults used in this study including 14 mainshocks in the Central-Taiwan-Mainshock sequence and 28 other surrounding earthquakes which are not in the sequence in Central Taiwan from 1900 to 2017. L: fault length in km. W: fault width in km. Unit of netslip is meter. "CWBSN" in the reference list indicates the location of the earthquake has obtained from the Central Weather Bureau Seismic Network. "CMT" indicates the focal mechanism information obtained from the global CMT catalog for specific earthquake. "BATS" stands for Broadband array in Taiwan for Seismology. Ref.: 1. (Liao et al. 2018); 2. (Lin et al. 2013); 3. (Lin & Xiao, 2004); 4. (Hsu et al. 2011); 5. (CWBSN, Kao et al., 2000); 6. (CWBSN, Wu, 1978); 7. (CWBSN, CMT); 8. (CWBSN, Ma & Wu, 2001); (9). (Hsu et al. 2009); (10). (CWBSN, Hsu et al., 2011); (11) (Lee et al., 2015); (12). (Lee et al., 2015); (13). (CWBSN, Wen et al., 2017); 14. (CMT); 15. (Ma & Wu, 2001); 16. (CWBSN); 17. (BATs); 18. (BATs, CMT).

No.	**Date**	**Lon**	**Lat**	**Depth**	**Strike**	**Dip**	**Rake**	**Fault Patch**			**M**	**Ref.**
								L	**W**	**netslip**		
Followings are 28 other surrounding earthquakes												
15	**1935/4/20**	**120.84**	**24.56**	**6**	**203**	**50**	**90**	**4.0**	**4.0**	**2.935**	**6.8**	**2**
16	**1986/5/20**	**121.29**	**23.79**	**37**	**214**	**45**	**67**	**14.0**	**8.7**	**0.605**	**6.2**	**7**
17	**1986/7/30**	**121.4**	**24.24**	**15**	**27**	**40**	**-111**	**5.7**	**4.9**	**0.236**	**5.5**	**14**
18	**1987/1/6**	**120.94**	**23.78**	**48.1**	**198**	**66**	**103**	**6.5**	**4.8**	**0.421**	**5.7**	**14**
19	**1988/4/7**	**121.21**	**23.6**	**18.9**	**39**	**64**	**97**	**5.6**	**4.3**	**0.392**	**5.6**	**14**
20	**1990/7/16**	**121.29**	**23.73**	**15**	**110**	**65**	**123**	**6.5**	**4.8**	**0.421**	**5.7**	**14**
21	**1991/1/18**	**121.27**	**23.68**	**0.79**	**125**	**16**	**-85**	**6.6**	**5.5**	**0.258**	**5.4**	**7**
22	**1993/12/15**	**120.51**	**23.19**	**15.21**	**200**	**48**	**84**	**6.5**	**4.8**	**0.421**	**5.65**	**15**
23	**1995/4/25**	**120.53**	**22.66**	**37.7**	**215**	**36**	**-39**	**5.7**	**4.9**	**0.236**	**5.5**	**16**
24	**1999/9/20**	**120.8763**	**23.7915**	**17**	**24.99**	**32.2**	**97.02**	**14.1**	**8.7**	**0.606**	**6.22**	**17**
25	**1999/9/20**	**121.0603**	**23.8502**	**24**	**303.3**	**49.15**	**6.52**	**12.0**	**7.7**	**0.563**	**6.1**	**17**
26	**1999/9/20**	**121.0387**	**23.8442**	**20**	**337.05**	**37.8**	**64.73**	**12.0**	**7.7**	**0.563**	**6.1**	**17**
27	**1999/9/20**	**120.82**	**23.6**	**19**	**246**	**89**	**179**	**19.1**	**11.0**	**0.700**	**6.4**	**18**
28	**1999/9/22**	**121.0467**	**23.8263**	**23**	**13.07**	**25.47**	**124.28**	**19.1**	**11.0**	**0.700**	**6.4**	**17**

Table S1. (continued) Fault parameters of all source faults used in this study including 14 mainshocks in the Central-Taiwan-Mainshock sequence and 28 other surrounding earthquakes which are not in the sequence in Central Taiwan from 1900 to 2017. L: fault length in km. W: fault width in km. Unit of netslip is meter. "CWBSN" in the reference list indicates the location of the earthquake has obtained from the Central Weather Bureau Seismic Network. "CMT" indicates the focal mechanism information obtained from the global CMT catalog for specific earthquake. "BATS" stands for Broadband array in Taiwan for Seismology. Ref.: 1. (Liao et al. 2018); 2. (Lin et al. 2013); 3. (Lin & Xiao, 2004); 4. (Hsu et al. 2011); 5. (CWBSN, Kao et al., 2000); 6. (CWBSN, Wu, 1978); 7. (CWBSN, CMT); 8. (CWBSN, Ma & Wu, 2001); (9). (Hsu et al. 2009); (10). (CWBSN, Hsu et al., 2011); (11) (Lee et al., 2015); (12). (Lee et al., 2015); (13). (CWBSN, Wen et al., 2017); 14. (CMT); 15. (Ma & Wu, 2001); 16. (CWBSN); 17. (BATs); 18. (BATs, CMT).

No.	**Date**	**Lon**	**Lat**	**Depth**	**Strike**	**Dip**	**Rake**	**Fault Patch**			**M**	**Ref.**
								L	**W**	**netslip**		
29	**1999/9/22**	**121.0245**	**23.7555**	**24**	**19.93**	**38.35**	**115.65**	**7.6**	**5.4**	**0.453**	**5.8**	**17**
30	**1999/9/23**	**121.07**	**23.93**	**21.1**	**193**	**62**	**100**	**5.6**	**4.3**	**0.392**	**5.6**	**16**
31	**1999/9/25**	**121.0058**	**23.8593**	**18**	**49.74**	**44.43**	**126.51**	**22.3**	**12.4**	**0.754**	**6.5**	**17**
32	**1999/10/22**	**120.46**	**23.48**	**18.8**	**46**	**52**	**125**	**7.6**	**5.4**	**0.453**	**5.8**	**7**
33	**1999/10/22**	**120.46**	**23.52**	**16**	**237**	**90**	**168**	**4.8**	**3.8**	**0.364**	**5.5**	**7**
34	**2000/2/15**	**120.75**	**23.32**	**18.5**	**52**	**69**	**123**	**5.6**	**4.3**	**0.392**	**5.6**	**16**
35	**2000/5/17**	**121.0975**	**24.193**	**13**	**91.45**	**21.08**	**170.28**	**5.6**	**4.3**	**0.392**	**5.6**	**17**
36	**2000/6/10**	**121.1092**	**23.901**	**27**	**201**	**82**	**96**	**19.1**	**11.0**	**0.700**	**6.4**	**18**
37	**2000/7/28**	**120.9327**	**23.411**	**12**	**353.95**	**62.89**	**10.85**	**5.6**	**4.3**	**0.392**	**5.6**	**17**
38	**2001/3/1**	**120.98**	**23.84**	**14.4**	**34**	**29**	**114**	**7.6**	**5.4**	**0.453**	**5.8**	**16**
39	**2009/11/5**	**120.76**	**23.77**	**23.3**	**194**	**56**	**116**	**5.6**	**4.3**	**0.392**	**5.6**	**16**
40	**2010/3/4**	**120.64**	**22.96**	**18.6**	**200**	**63**	**160**	**6.5**	**4.8**	**0.421**	**5.7**	**16**
41	**2012/2/26**	**120.74**	**22.72**	**32.3**	**188**	**69**	**113**	**16.4**	**9.8**	**0.651**	**5.9**	**16**
42	**2013/3/7**	**121.47**	**24.31**	**1.4**	**28**	**56**	**82**	**8.8**	**6.1**	**0.487**	**5.9**	**16**

Table S2. ΔCFS as induced by preceding mainshocks in the Central-Taiwan-Mainshock earthquake sequence at hypocenter of each subsequent mainshock. Unit is bar for the calculated ΔCFS. Events in the top row are the source faults, whereas events in the left column mark the receiver faults. The local magnitudes (M_L) of mainshocks in the sequence are shown in the top row. 2013M: 2013 Nantou earthquake in March; 2013J: 2013 Nantou earthquake in June. The other twelve events are the same as listed in Table 1.

Event	**1906 (6.9)**	**1935 (7.1)**	**1941 (7.3)**	**1946 (6.1)**	**1964 (6.3)**	**1972 (6.1)**	**1983 (6.0)**	**1998 (6.2)**	**1999 (7.3)**	**2009 (6.2)**	**2010 (6.4)**	**2013M (6.2)**	**2013J (6.5)**	**Total**
1935	-0.21													-0.21
1941	-0.28	0												-0.28
1946	-0.88	-0.15	-0.04											-1.07
1964	0.08	0.01	5.81	0.03										5.93
1972	-0.06	0.51	-0.10	0	0									0.35
1983	-0.05	0.34	-0.03	0	0	0								0.26
1998	-2.26	0.07	-13.63	0	0	0	0							-15.82
1999	0.06	0.25	0.41	0	0	0	0	0						0.72
2009	0.36	-0.98	0.79	0	0	0	0	0	-0.72					-0.55
2010	-0.02	-0.02	0.24	0.02	0	0	0	0	0.07	0				0.29
2013M	0.05	0.33	0.07	0	0	-0.08	0	0	11.85	-0.01	0			12.21
2013J	0.16	0.21	0.18	0	0	-0.04	0	0	2.14	0.03	0	1.40		4.08
2016	-0.19	-0.03	-0.28	0.24	0	0	0	0	-0.07	0	0.54	0	0	0.21

Table S3. Standard deviation for each tested parameter, overall standard deviation resulted from all parameters and percentages of their contributions to the overall standard deviation for two sensitivity analyses: 1999 Chi-Chi and 2009 Nantou vs 1999 Chi-Chi and 2010 Jiashian.

Tested Parameter	**Sensitivity Analysis between 1999 Chi-Chi and 2009 Nantou**		**Sensitivity Analysis between 1999 Chi-Chi and 2010 Jiashian**	
	Standard Deviation	**Percentage of Their Contributions**	**Standard Deviation**	**Percentage of Their Contributions**
Source Slip Models	0.12	18.87%	0	0%
Strike of Receiver Fault	0.05	3.28%	0.01	14.28%
Dip of Receiver Fault	0.07	6.42%	0.01	14.28%
Rake of Receiver Fault	0.03	1.18%	0	0%
Epicenter	0.14	25.69%	0.01	14.28%
Focal Depth	0.14	25.69%	0	0%
Effective Friction Coefficient	0.12	18.87%	0.02	57.16%
All Parameters	0.28	100%	0.02	100%

Table S4. Occurrence times, hypocenters, source mechanisms, moment magnitude of the 9 earthquakes outside our study area. The numbers in the Ref. Column correspond to: (1) (Chung et al., 2008); (2) (Yu & Liu, 1986); (3) (Hwang & Kanamori, 1989); (4) (Wu et al., 2009).

Event	Hypocenter			Source Mechanisms				Ref.
Date	Lon	Lat	Depth	Strike	Dip	Rake	M	
1951/10/21	121.73	23.88	4	25	85	31	7.3	(1)
1951/10/22 03:29:31	121.73	24.08	1	25	85	73	7.1	(1)
1951/10/22 05:42:58	121.95	23.83	16	45	75	60	7.1	(1)
1951/11/24 18:47:23	121.23	23.10	16	32	70	70	6.8	(1)
1951/11/24 18:50:30	121.35	23.28	36	25	70	40	7.1	(1)
1986/05/20	121.592	24.082	16	35	60	90	6.5	(2)
1986/11/14	121.833	23.992	13.9	43	57	100	6.8	(3)
2006/12/26 12:26:20.9	120.494	21.754	50.9	165	30	-76	7.0	(4)
2006/12/26 12:34:14.7	120.410	21.995	41.0	151	48	0	7.0	(4)

Table S5. Calculated ΔCFS due to preceding earthquakes (42 events) within the polygon, due to 9 events outside the polygon, due to total 51 (42 + 9) events and outcome of the analysis, which described in the following terms: Earthquake promotion (P; ΔCFS ≥ 0.1 bar), Earthquake inhibition (I; ΔCFS ≤ -0.1 bar), and neutral (N; -0.1 < ΔCFS < 0.1 bar). In the outcome of analysis, no change means no magnitude change after adding 9 events' effect, slight increase or decrease means absolute value of magnitude change is smaller than 0.1 bar, increase or decrease means absolute value of magnitude change is larger than 0.1 bar.

Receiver fault	ΔCFS due to preceding events (42) within the polygon	ΔCFS due to 9 events outside the polygon	ΔCFS due to total 51 events	Analysis outcome: Promoted (P), Inhibited (I), or Neutral (N)
1906/3/16	-	-	-	-
1935/4/20	-0.21	-	-0.21	I (no change)
1941/12/16	-0.28	-	-0.28	I (no change)
1946/12/4	-1.07	-	-1.07	I (no change)
1964/1/18	5.93	0.01	5.94	P (slight increase)
1972/11/9	0.38	-0.20	0.180	P (decrease)
1983/5/11	0.53	0.35	0.88	P (increase)
1998/7/17	-15.81	-0.11	-15.92	I (slight decrease)
1999/9/20	0.74	-0.06	0.68	P (slight decrease)
2009/11/5	-1.26	-0.04	-1.30	I (slight decrease)
2010/3/4	0.28	0.09	0.37	P (slight increase)
2013/3/27	-4.71	-0.01	-4.72	I (slight decrease)
2013/6/2	-38.49	-0.02	-38.51	I (slight decrease)
2016/2/5	0.10	-0.08	0.02	N

Table S6. Calculated Coulomb stress change due to coseismic effects of preceding earthquakes, 1999 Chi-Chi coseismic effect only, 1999 postseismic afterslip effect only, coseismic of preceding earthquakes and 1999 postseismic afterslip in total and analysis of the outcome after considering 1999 postseismic afterslip at hypocenters of subsequent mainshocks in the sequence. The outcome of the analysis is described in the following terms: Earthquake promotion (P; ΔCFS ≥ 0.1 bar), Earthquake inhibition (I; ΔCFS ≤ -0.1 bar), and neutral (N; -0.1 < ΔCFS < 0.1 bar). In the outcome of analysis, no change means no magnitude change after adding postseismic effect, slight increase or decrease means absolute value of magnitude change is smaller than 0.1 bar, increase or decrease means absolute value of magnitude change is larger than 0.1 bar.

Receiver fault	ΔCFS due to preceding events	ΔCFS due to 1999 coseismic	ΔCFS due to 1999 postseismic afterslip	ΔCFS due to coseismic and postseismic afterslip	Analysis outcome: Promoted (P), Inhibited (I), or Neutral (N)
2009/11/5	-1.26	-0.72	-0.16	-1.42	I (decrease)
2010/3/4	0.28	0.07	-0.01	0.27	P (slight decrease)
2013/3/27	-4.71	11.85	-0.40	-5.11	I (decrease)
2013/6/2	-38.49	2.14	-0.58	-39.07	I (decrease)
2016/2/5	0.10	-0.07	0.01	0.11	P (slight increase)

Captions:

Figure S1. Coulomb stress change on nearby active faults and rupture planes of subsequent mainshocks before each subsequent mainshock in the Central-Taiwan-Mainshock sequence ((a) – (l)). The dark dot in each subplot shows the epicenter of each subsequent mainshock. CHF: Changhua fault; CLPF: Chelungpu Fault; STF: Shungtung Fault; FDCT: Flat Decollement of Central Taiwan; CKF: Chukou Fault; HHF: Hsinghua Fault; CCF: Chaochou Fault; CSF: Chishan Fault.

Figure S2. Snapshot of Coulomb stress change due to preceding earthquakes from 1900 to 2017 on each major active fault: (a) Changhua Fault; (b) Chelungpu Fault; (c) Flat decollement of Central Taiwan; (d) Shungtung Fault; (e) Chukou Fault; (f) Chishan Fault; (g) Chaochou Fault; (h) Hsinhua Fault. CHF: Changhua Fault; CLPF: Chelungpu Fault; STF: Shungtung Fault; FDCT: Flat Decollement of Central Taiwan; CKF: Chukou Fault; HHF: Hsinghua Fault; CCF: Chaochou Fault; CSF: Chishan Fault.

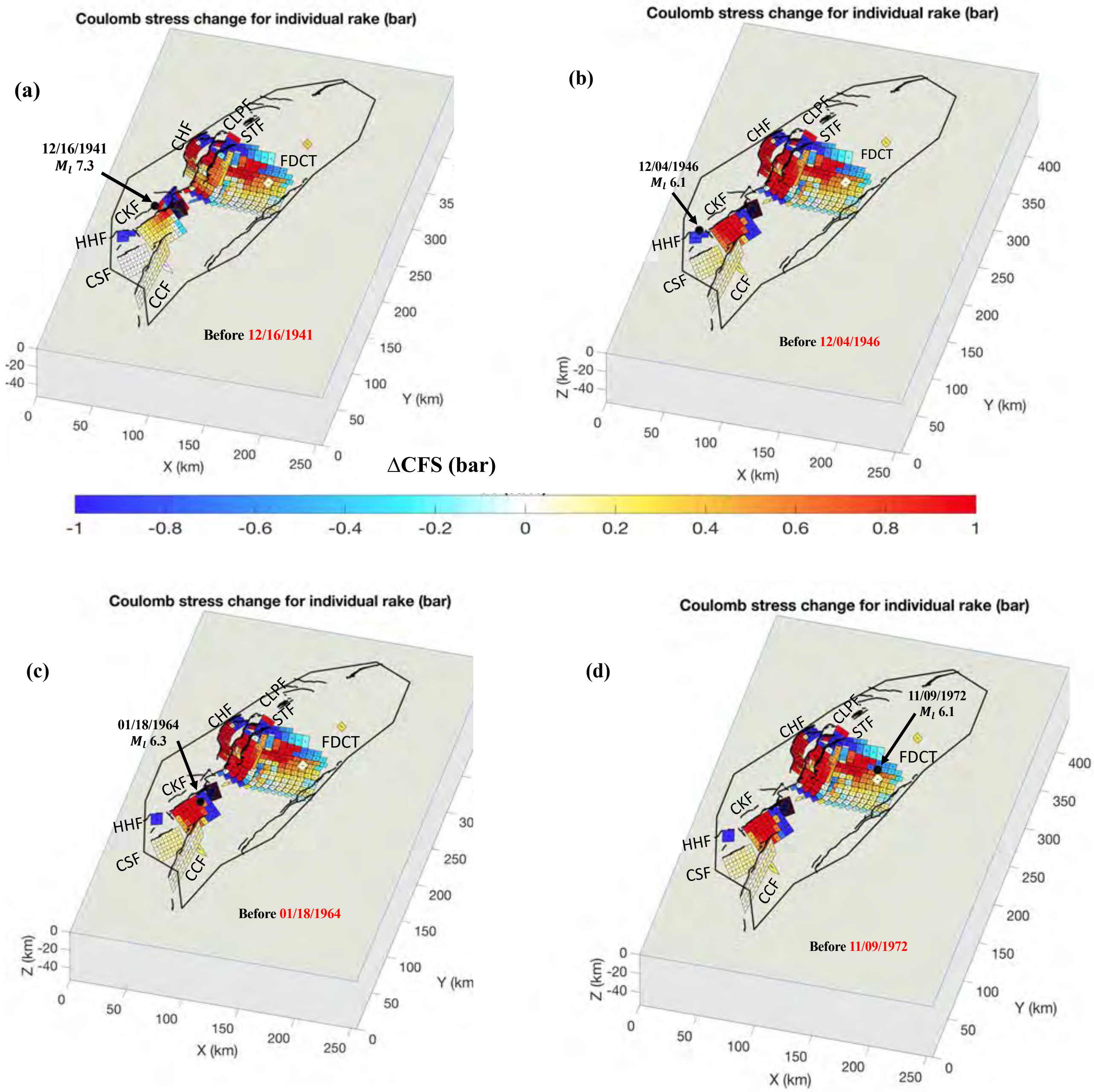
Coulomb stress change for individual rake (bar)
(a)
12/16/1941
M_l 7.3
CHF
CLPF
STF
FDCT
CKF
HHF
CSF
CCF
Before 12/16/1941
(b)
12/04/1946
M_l 6.1
Before 12/04/1946
ΔCFS (bar)
(c)
01/18/1964
M_l 6.3
Before 01/18/1964
(d)
11/09/1972
M_l 6.1
Before 11/09/1972
X (km)
Y (km)
Z (km)

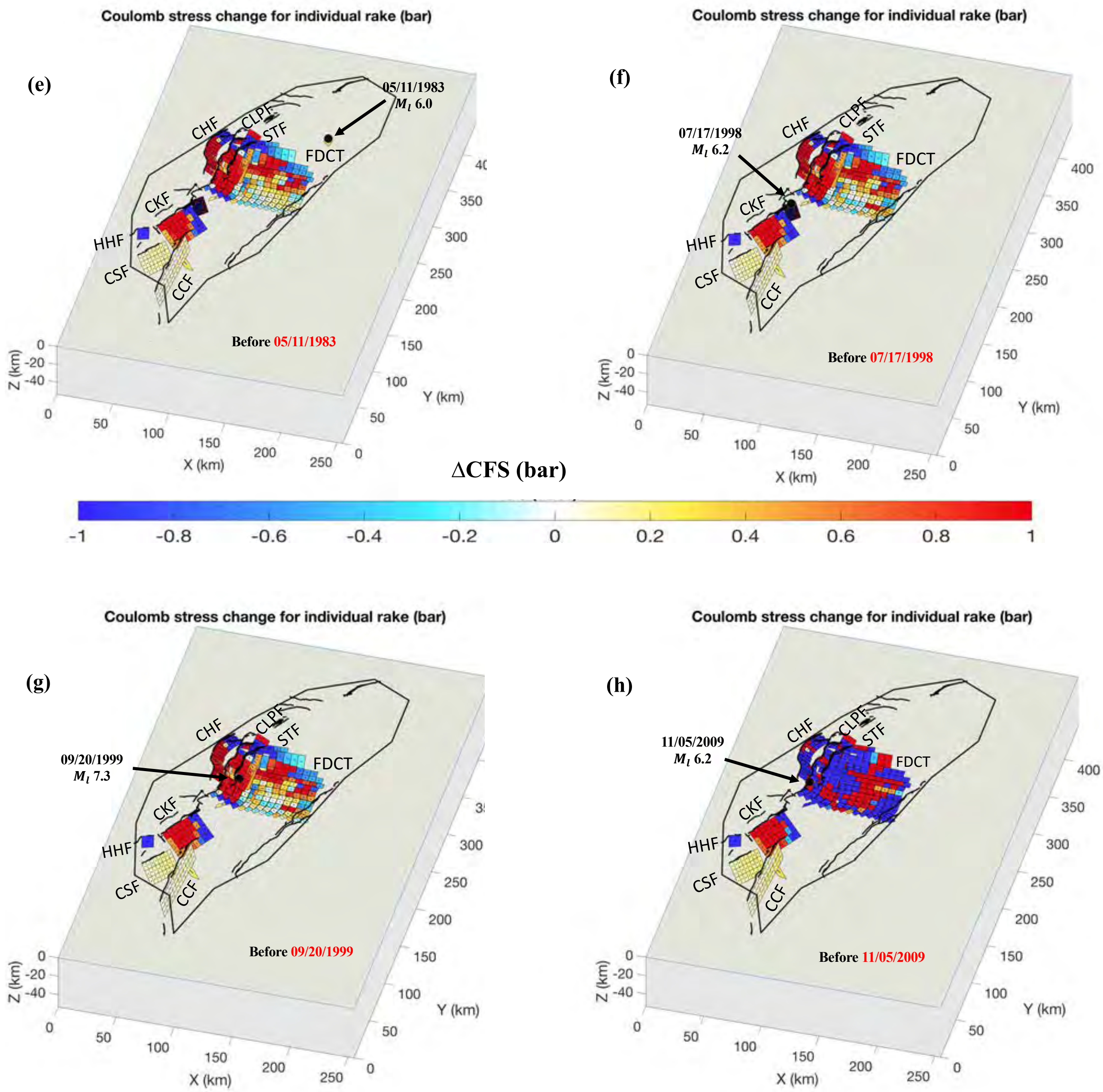
Coulomb stress change for individual rake (bar)
(e)
05/11/1983
M_l 6.0
CHF
CLPF
STF
FDCT
CKF
HHF
CSF
CCF
Before 05/11/1983
Z (km)
X (km)
Y (km)
Coulomb stress change for individual rake (bar)
(f)
07/17/1998
M_l 6.2
Before 07/17/1998
ΔCFS (bar)
-1
-0.8
-0.6
-0.4
-0.2
0
0.2
0.4
0.6
0.8
1
Coulomb stress change for individual rake (bar)
(g)
09/20/1999
M_l 7.3
Before 09/20/1999
Coulomb stress change for individual rake (bar)
(h)
11/05/2009
M_l 6.2
Before 11/05/2009

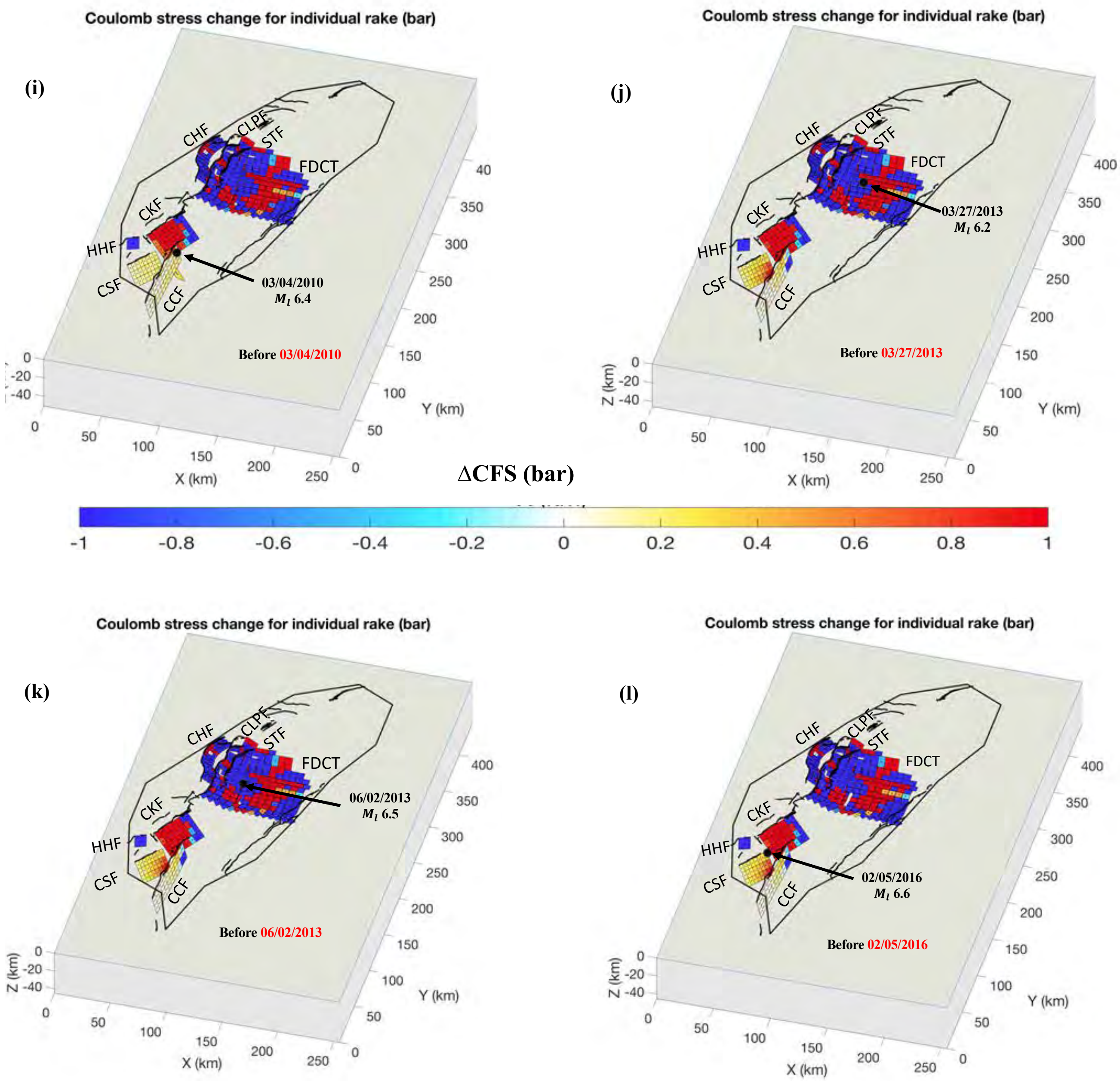

Coulomb stress change for individual rake (bar)
(i)
CHF
CLPF
STF
FDCT
CKF
HHF
CSF
CCF
03/04/2010
M_L 6.4
Before 03/04/2010
Coulomb stress change for individual rake (bar)
(j)
03/27/2013
M_L 6.2
Before 03/27/2013
Z (km)
X (km)
Y (km)
ΔCFS (bar)
-1
-0.8
-0.6
-0.4
-0.2
0
0.2
0.4
0.6
0.8
1
Coulomb stress change for individual rake (bar)
(k)
06/02/2013
M_L 6.5
Before 06/02/2013
Coulomb stress change for individual rake (bar)
(l)
02/05/2016
M_L 6.6
Before 02/05/2016

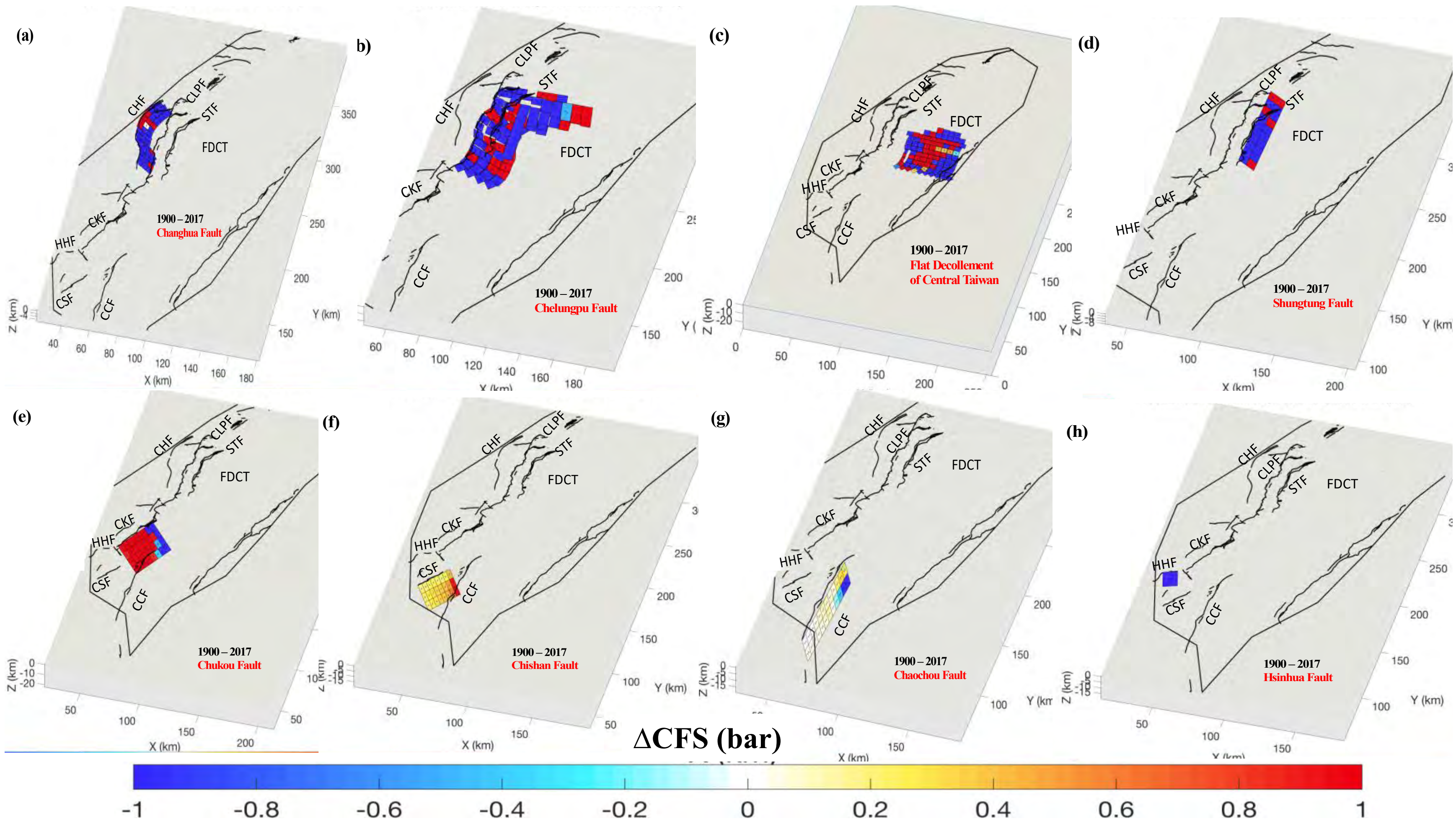

(a)
1900 – 2017
Changhua Fault
b)
1900 – 2017
Chelungpu Fault
(c)
1900 – 2017
Flat Decollement of Central Taiwan
(d)
1900 – 2017
Shungtung Fault
(e)
1900 – 2017
Chukou Fault
(f)
1900 – 2017
Chishan Fault
(g)
1900 – 2017
Chaochou Fault
(h)
1900 – 2017
Hsinhua Fault
CHF
CLPF
STF
FDCT
CKF
HHF
CSF
CCF
X (km)
Y (km)
Z (km)
ΔCFS (bar)
-1
-0.8
-0.6
-0.4
-0.2
0
0.2
0.4
0.6
0.8
1